Bimetallic Reactivity. Oxo Transfer Reactions with a Heterobimetallic Complex of Iron(II) and Vanadium(III)

David G. McCollum,[†] Glenn P. A. Yap,[‡] Louise Liable-Sands,[‡] Arnold L. Rheingold,[‡] and B. Bosnich*,[†]

Department of Chemistry, The University of Chicago, 5735 South Ellis Avenue, Chicago, Illinois 60637, and Department of Chemistry and Biochemistry, University of Delaware, Newark, Delaware 19716

Received August 14, 1996

Many multimetallic proteins employ the reducing potential of two or more proximal metals for the multielectron reduction of substrates.[1] For example, laccase[2] employes four copper ions for the reduction of dioxygen to water. Although the dioxygen appears to bind to two of the copper ions, all four copper ions act in the four electron reduction process.[3] Similarly hemerythrin, where two contiguous iron(II) ions are present, binds dioxygen to only one of the metals but uses the reducing power of both to convert dioxygen to peroxide[4] (eq 1). Although such multielectron reductions are common in metalloproteins, the process is seldom observed in synthetic multimetallic systems.[5] It is more usual to observe that, in bimetallic systems, the oxidation of one of the metals leads to the deactivation of the other.[6,7] A notable example of this mutual deactivation is the

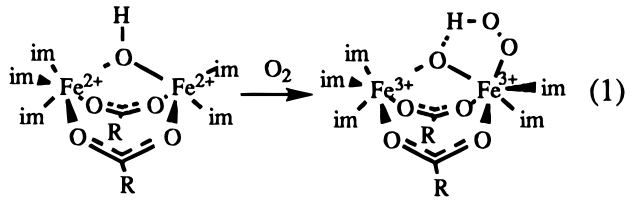

(1)

case of the symmetrical dirhodium(I) dimer which undergoes oxidative addition of H_2 to only one rhodium atom (eq 2).

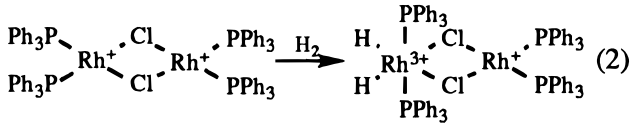

(2)

Although the hemerythrin O_2 oxidative addition (eq 1) and the putative double H_2 addition to the rhodium dimer are not strictly analogous because the former requires electron transfer between metals, they resemble each other by the requirement that both metals be oxidized. This difference in behavior between the two dimers raises questions about the origins of the mutual deactivation in bimetallic complexes. This paper deals with these questions by investigating two-metal oxidations in heterobimetallic systems.

The ligands used in these investigations are shown in **1** and **2**.[8−13] Both of these ligands have two metal-binding sites, one

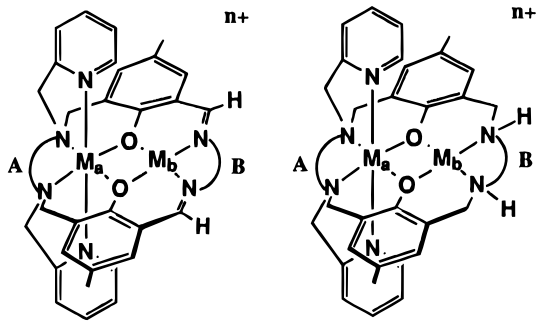

1 **2**

6-coordinate (closed site) and one 4-coordinate (open site). The purpose of this design is to allow a substrate, such as O_2, to bind to the open site but to be reduced by both metals. Thus, for example, it is conceivable that, for a dicobalt(II) complex, binding of O_2 to the open-site cobalt(II) could lead to the formation of a dicobalt(III) peroxide complex, in analogy to the process encountered in hemerythrin. There are clearly other two-electron reductions which can be envisioned with these systems using other substrates. The ligand systems **1** and **2** differ by the presence of imine (im) or amine (am) groups in the open site. The links A and B can consist of either two (en)

[†] The University of Chicago.
[‡] University of Delaware.

(1) Hemocyanin: (a) Karlin, K. D.; Tyeklár, Z. *Bioinorganic Chemistry of Copper*; Chapman & Hall: New York, 1993. (b) Kitajima, N.; Moro-oka, Y. *Chem. Rev.* **1994**, *94*, 737−57. (c) Magnus, K. A.; Hazes, B.; Ton-That, H.; Bonaventura, C.; Bonaventura, J.; Hol, W. G. J. *Proteins: Struct., Funct., Genet.* **1994**, *19*, 302−9. (d) Ling, J.; Nestor, L. P.; Czernusewicz, R. S.; Spiro, T. G.; Fraczkiewicz, R.; Sharma, K. D.; Loehr, T. M.; Sanders-Loehr, J. *J. Am. Chem. Soc.* **1994**, *116*, 7682−91. (e) Jung, B.; Karlin, K. D.; Zuberbühler, A. D. *J. Am. Chem. Soc.* **1996**, *118*, 3763−4. (f) Halfen, J. A.; Mahapatra, S.; Wilkinson, E. C.; Kaderli, S.; V. G. Young, J.; L. Que, J.; Zuberbühler, A. D.; Tolman, W. B. *Science* **1996**, *271*, 1387−1400. Ascorbate oxidase: (g) Messerschmidt, A.; Luecke, H.; Huber, R. *J. Mol. Biol.* **1993**, *230*, 997−1014. (h) Messerschmidt, A.; Ladenstein, R.; Huber, R.; Bolognesi, M.; Avigliano, L.; Petruzelli, R.; Rossi, A.; Finazzi-Agró, A. *J. Mol. Biol.* **1992**, *224*, 179−205. (i) Messerschmidt, A.; Rossi, A.; Ladenstein, R.; Huber, R.; Bolognesi, M.; Gatti, G.; Marchesini, A.; Petruzelli, R.; Finazzo-Agró, A. *J. Mol. Biol.* **1989**, *206*, 513−29. Cytochrome *c*: (j) Tsukihara, T.; Aoyama, H.; Yamashita, E.; Tomizaki, T.; Yamaguchi, H.; Shinzawa-Itoh, K.; Nakashima, R.; Yaono, R.; Yoshikawa, S. *Science* **1995**, *269*, 1069−74. (k) Babcock, G. T.; Wikström, M. *Nature* **1992**, *356*, 301−9. (l) Fox, S.; Nanthakumar, A.; Wilkström, M.; Karlin, K. D.; Blackburn, N. J. *J. Am. Chem. Soc.* **1996**, *118*, 24−34. (m) Scott, M. J.; Zhang, H. H.; Lee, S. C.; Hedman, B.; Hodgson, K. O.; Holm, R. H. *J. Am. Chem. Soc.* **1995**, *117*, 568−9. Dinuclear iron proteins: (n) Wilkins, R. G. *Chem. Soc. Rev.* **1992**, 171−8. (o) Feig, A. L.; Lippard, S. J. *Chem. Rev.* **1994**, *94*, 759−805. (p) Howard, J. B.; Rees, D. C. *Adv. Protein Chem.* **1991**, *42*, 199−280.

(2) Laccase: (a) Solomon, E. I.; Lowery, M. D. *Science* **1993**, *259*, 1575−81. (b) Cole, J. L.; Clark, P. A.; Solomon, E. I. *J. Am. Chem. Soc.* **1990**, *112*, 9534−48.

(3) Shin, W.; Sundaram, U. M.; Cole, J. L.; Zhang, H. H.; Hedman, B.; Hodgson, K. O.; Solomon, E. I. *J. Am. Chem. Soc.* **1996**, *118*, 3202−15.

(4) Hemerythrin: (a) Stenkamp, R. E. *Chem. Rev.* **1994**, *94*, 715−27. (b) Solomon, E. I.; Zhang, Y. *Acc. Chem. Res.* **1992**, *25*, 343−52. (c) Holmes, M. A.; Trong, I. L.; Turrey, S.; Steker, L. C.; Stenkamp, R. E. *J. Mol. Biol.* **1991**, *218*, 583−93.

(5) Halpern, J.; Goodall, B. L.; Khare, G. P.; Lim, H. S.; Pluth, J. J. *J. Am. Chem. Soc.* **1975**, *97*, 2301−3.

(6) Schenck, T. G.; Downes, J. M.; Milne, C. R. C.; Mackenzie, P. B.; Boucher, H.; Whelan, J.; Bosnich, B. *Inorg. Chem.* **1985**, *24*, 2334−7.

(7) Schenck, T. G.; Milne, C. R. C.; Sawyer, J. F.; Bosnich, B. *Inorg. Chem.* **1985**, *24*, 2338−44.

(8) Fraser, C.; Johnston, L.; Rheingold, A. L.; Haggerty, B. S.; Williams, G. K.; Whelan, J.; Bosnich, B. *Inorg. Chem.* **1992**, *31*, 1835−44.

(9) Fraser, C.; Ostrander, R.; Rheingold, A. L.; White, C.; Bosnich, B. *Inorg. Chem.* **1994**, *33*, 324−37.

(10) Fraser, C.; Bosnich, B. *Inorg. Chem.* **1994**, *33*, 338−44.

(11) McCollum, D. G.; Hall, L.; White, C.; Ostrander, R.; Rheingold, A. L.; Whelan, J.; Bosnich, B. *Inorg. Chem.* **1994**, *33*, 924−33.

(12) McCollum, D. G.; Fraser, C.; Ostrander, R.; Rheingold, A. L.; Bosnich, B. *Inorg. Chem.* **1994**, *33*, 2383−92.

(13) McCollum, D. G.; Yap, G. P. A.; Rheingold, A. L.; Bosnich, B. *J. Am. Chem. Soc.* **1996**, *118*, 1365−79.

S0020-1669(96)00992-5 CCC: $14.00

or three (tn) methylene groups. The nomenclature for the ligands identifies the closed-site link first, followed by the open-site link, followed by the designation im or am. Thus, for example, the ligand with a dimethylene A link and a trimethylene B link with diimine groups is written as entnim. For the complexes, the closed-site metal is written first, followed by the ligand, followed by the open-site metal, followed by the ligands attached to the open-site metal. For example, the heterobimetallic zinc−cobalt complex of the entnim ligand is written as $[Zn(entnim)CoX]^+$.

We recently reported[13] that when one of the metals in dicobalt(II) complexes formed from the amine ligands, **2**, was oxidized, the other metal was deactivated to oxidation despite the fact that either site was capable of supporting the higher Co(III) oxidation state. In order to demonstrate that this mutual deactivation is not metal dependent, we have investigated the oxidation of an iron(II)−vanadium(III) system with an oxo transfer reagent. This system was chosen because of the anticipated thermodynamic stability of Fe(III) in the closed site and of the vanadyl ion in the open site. The two-metal oxidation is expected to occur by the sequential electron transfer illustrated in eq 3. Further, the formation of a V^{5+}−oxo intermediate would provide a strong kinetic driving force for the production of the $Fe^{III}-V^{IV}O$ product.

$$[Fe^{II}(L)V^{III}Cl_2]^+ \xrightarrow{[O]} [Fe^{II}(L)V^{V}(O)Cl]^{2+} \rightarrow [Fe^{III}(L)V^{IV}O]^{3+} \quad (3)$$

1. Synthesis. Monometallic iron(II) complexes were prepared by the methods outlined in eq 4. The preparation of the (solid) dialdehyde **3** has been reported previously.[8,13] Reaction with $[Fe(py)_4Cl_2]$[14] gives **4**, which, in turn, can be cyclized with a diamine in the presence of acetic acid to give the monometallic diprotonated complex **5**. By this method, 60−80% yields of brown crystals of $[Fe(entnim)(H^+)_2](PF_6)_2$, $[Fe(tnenim)(H^+)_2](PF_6)_2$, and $[Fe(tntnim)(H^+)_2](PF_6)_2$ were isolated. These solid spin-free monometallic iron(II) complexes are indefinitely stable in air but are slowly oxidized in air when dissolved in CH_3CN solutions. The corresponding amine complexes were prepared by BH_4^- reduction by the method outlined in eq 5. In this way $[Fe(entnam)(H^+)_2](PF_6)_2$ was isolated as yellow crystals, and $[Fe(tntnam)(H^+)_2](PF_6)_2$ formed pale green crystals. Unlike the corresponding imine complexes, these amine complexes are extremely air sensitive as solids, and their yellow CH_3CN solutions are oxidized by O_2 upon exposure to air to give deep blue solutions. Iron(III) phenolate complexes are deep blue in color because of a Fe(III)−phenolate charge transfer band,[15] and the appearance of the blue color is a sensitive test for the presence of iron(III). The monometallic iron(II) amine complexes are also spin-free. The diiron(II) complex $[Fe(entnim)FeCl]PF_6$ was prepared by the method outlined in eq 6. The maroon crystals of the product are indefinitely air stable in the solid state and in CH_3CN solutions. The 25 °C magnetic moment for the dimer is 7.09 μ_B, indicating slight magnetic exchange between the iron(II) ions. The corresponding orange amine complex, $[Fe(entnam)FeCl]^+$, is extremely air sensitive. It was prepared in CH_3CN solutions by the addition of $FeCl_2$ and DBU[16] to $[Fe(entnam)(H^+)_2]^{2+}$, but it was not isolated.

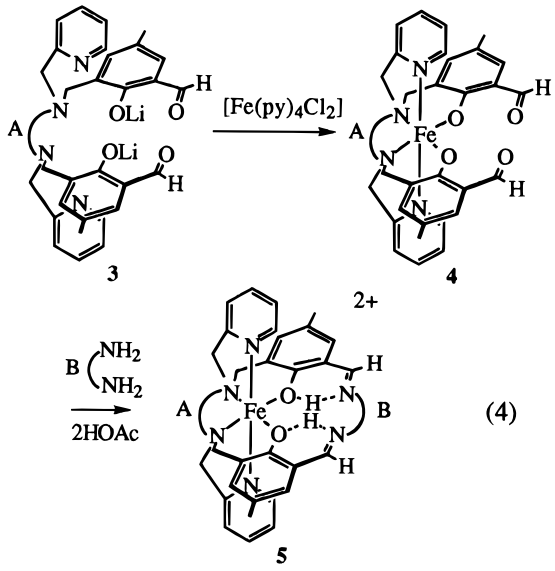

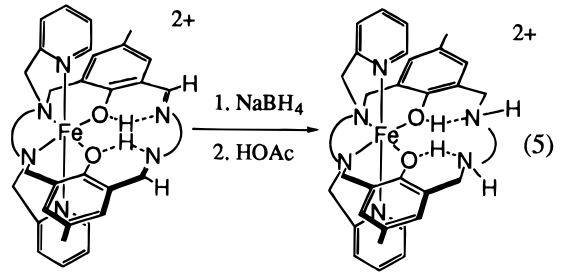

$$[Fe(entnim)(H^+)_2](PF_6)_2 \xrightarrow{[Fe(py)_4Cl_2]} [Fe(entnim)FeCl]PF_6 \quad (6)$$

The redox chemistry of these iron(II) complexes was investigated by cyclic voltammetry and by chemical means. The addition of 1 equiv of ferrocenium ions (fc^+) to $[Fe(entnim)(H^+)_2]^{2+}$ in CH_3CN solutions led to the immediate reduction of fc^+ and the production of a deep blue solution of the complex characteristic of iron(III) phenolate complexes. The homologous complex $[Fe(tnenim)(H^+)_2]^{2+}$ was not oxidized by fc^+ under the same conditions. This behavior is analogous to that observed with the corresponding cobalt(II) complexes,[13] where fc^+ only causes oxidation when the en link is present in the closed site. Similarly, we find that all of the monometallic iron(II) amine complexes are immediately oxidized by O_2 irrespective of whether an en or tn link is present in the closed site. For the case of the oxidation of the monometallic cobalt(II) complexes, it was argued[13] that the required bond length contraction associated with oxidation was resisted by the presence of the rigid imine groups. It was assumed that the larger bite angle of the tn link required greater conformational accommodation than the en link. A similar conformational restraint appears to apply for the present iron complexes, where all of the less rigid amine ligands are readily oxidized but only the iron complexes with a closed-site en link are oxidized for the imine ligands. It is probable that the conformational effects are more pronounced with the cobalt(III) complexes than those of iron(III) because the former demand a more rigid and defined geometry, which allows the ligand less conformational freedom. The conformational effects on the redox potentials are referred to as mechanical coupling[13] because, in principle, the conformational adjustments could be calculated by molecular mechanics.

The diiron(II) complexes introduce new considerations for their oxidations. The addition of 1 equiv of fc^+ to either the $[Fe(entnim)FeCl]^+$ or the $[Fe(entnam)FeCl]^+$ complex in CH_3-

(14) Baudisch, O.; Hartung, W. H. *Inorg. Synth.* **1939**, *1*, 184−5.
(15) (a) Lever, A. B. P. *Inorganic Electronic Spectroscopy*, 2nd ed.; Elsevier: New York, 1984; Chapter 5. (b) Nanda, K. K.; Dutta, S. K.; Baitalik, S.; Venkatsubramanian, K.; Nag, K. *J. Chem. Soc., Dalton Trans.* **1995**, 1239−44. (c) Murch, B. P.; Bradley, F. C.; Que, L., Jr. *J. Am. Chem. Soc.* **1986**, *108*, 5027−8.
(16) DBU = 1,8-diazabicyclo[5.4.0]undec-7-ene.

Table 1. Redox Potentials and Peak Separations for the Fe^{III}/Fe^{II} Couples of Monometallic and Bimetallic Complexes[a,b]

complex	E_f, V	$E_{pa} - E_{pc}$, V
$[Fe(entnim)(H^+)_2]^{2+}$	−0.15	0.059
$[Fe(tnenim)(H^+)_2]^{2+}$	+0.03	0.060
$[Fe(tntnim)(H^+)_2]^{2+}$	−0.01	0.060
$[Fe(entnam)(H^+)_2]^{2+}$	−0.51	0.081
$[Fe(tntnam)(H^+)_2]^{2+}$	−0.40	0.069
$[Fe(entnim)FeCl]^+$	+0.69	0.082
	−0.16	0.067

[a] Conditions: 5×10^{-4} M sample, 0.1 M *n*-Bu_4NPF_6 in CH_3CN; Pt button working electrode; Pt wire auxiliary electrode; $Ag/AgNO_3$ nonaqueous or Ag wire reference electrode. [b] Potentials are reported relative to the ferrocenium/ferrocene (fc^+/fc) couple as an internal or external standard which is assigned a value of 0.00 V.

CN solutions gives an intense blue solution characteristic of iron(III)−phenolate complexes. The addition of another 1 equiv of fc^+ to these solutions does not cause further oxidation. Thus it appears that, after the oxidation of the first iron atom, the other is deactivated to oxidation, as was reported previously[13] for the dicobalt(II) complexes of these ligands.

The redox potentials of the iron(II) complexes relative to the fc^+/fc couple are listed in Table 1. The results are consistent with the described chemical oxidations. For the three monometallic complexes, the two with tn links in the closed site have more positive potentials than those where an en link is present in the same site. Reduction of the imine groups to amines leads to monometallic complexes which have redox potentials considerably more negative, by about 0.4 V. This observation provides strong evidence that conformational flexibility of the ligand has a strong influence on the redox potential. The $[Fe(entnim)FeCl]^+$ complex shows two reversible waves which are separated by 0.85 V. Because the −0.16 V wave is essentially the same as the potential of the $[Fe(entnim)(H^+)_2]^+$ complex, we assume that this couple is associated with the closed-site iron atom. Similarly, we conclude that the fc^+ oxidation of the $[Fe(entnim)FeCl]^+$ complex described earlier involves oxidation of the closed-site iron atom. This is probably also the case when the $[Fe(entnam)FeCl]^+$ complex is oxidized by fc^+. The ligand environment about the open-site iron(II) would be expected to allow for ready oxidation to the iron(III) state[17] in a monometallic complex. The fact that the open-site iron(II) in the bimetallic complex $[Fe(entnim)FeCl]^+$ has a large positive potential suggests that special forms of deactivation exist in bimetallic complexes.

2. Iron−Vanadium Complexes. Reaction of the $[Fe(entnim)(H^+)_2](PF_6)_2$ complex with VCl_3·3THF in CH_3CN solution in the presence of triethylamine leads to the formation of orange crystals of $[Fe(entnim)(\mu\text{-}Cl)VCl]PF_6$. One of the chloro ligands (μ-Cl) bridges the iron and vanadium metals. These crystals appear to be indefinitely stable in air in the solid state. So far we have been unable to isolate, in pure form, $Fe^{II}-V^{III}$ complexes of the other imine ligands or of the corresponding amine ligands.

When the $[Fe(entnim)(\mu\text{-}Cl)VCl]PF_6$ is suspended in CH_3CN and allowed to react with 2,4,6-trimethyliodosobenzene, the solution slowly turns green; green crystals of a complex of the formula $[Fe(entnim)VO](PF_6)_2$ are isolated from this solution. This same complex is isolated by two other means starting from $[Fe(entnim)(\mu\text{-}Cl)VCl]PF_6$. When $[Fe(entnim)(\mu\text{-}Cl)VCl]PF_6$ is dissolved in CH_3CN and exposed to O_2, the solution rapidly turns yellow and then over a period of days becomes green; $[Fe(entnim)VO](PF_6)_2$ is isolated from this solution. Similarly, addition of 1 equiv of fc^+ to $[Fe(entnim)(\mu\text{-}Cl)VCl]PF_6$ in CH_3CN solution gives a red solution;[18] which upon exposure to moisture produces the green complex, $[Fe(entnim)VO]^{2+}$. Addition of 2 equiv of fc^+ to $[Fe(entnim)(\mu\text{-}Cl)VCl]^+$ gives the same product with 1 equiv of fc^+ remaining. All of the physical properties (see Experimental Section) of $[Fe(entnim)VO](PF_6)_2$ indicate that it is an $iron^{II}-vanadium^{IV}$ complex. Reaction of $[Fe(entnim)(\mu\text{-}Cl)VCl]^+$ with the oxo transfer reagent probably leads to the initial formation of a vanadium(V) oxo species $[Fe^{II}(entnim)V^{V}O]^{2+}$, which might be expected to give a $Fe^{III}-V^{IV}O$ complex if the redox potential of iron in the closed site were the same as that found for the $[Fe(entnim)(H^+)_2]^{2+}$ and $[Fe(entnim)FeCl]^+$ complexes (Table 1). Intramolecular electron transfer does not occur; rather some form of intermolecular electron transfer appears to occur to give the thermodynamically stable Fe^{II} to $V^{IV}O$ complex. The reaction with O_2 presumably leads to a peroxo vanadium(V) species rather than a $Fe^{III}-V^{IV}$ peroxo product. Because the iron(II) in the closed site does not appear to be readily oxidized, the putative vanadium(V) peroxo species decomposes to the vanadyl complex by an unknown process. Oxidation of $[Fe(entnim)(\mu\text{-}Cl)VCl]^+$ with fc^+ probably leads to the formation of a $Fe^{II}-V^{IV}$ complex,[18] which, upon exposure to water, leads to the formation of the $Fe^{II}-V^{IV}O$ product. This behavior is not restricted to $Fe^{II}-V^{III}$ complexes; it also occurs with the analogous $Co^{II}-V^{III}$ complex, $[Co(entnim)VCl_2]^+$, which upon addition of the oxo transfer reagent gives the air stable tan complex $[Co^{II}(entnim)V^{IV}O]^{2+}$.

The deactivation of the closed-site metal to oxidation is revealed in the electrochemical data in Table 2. For the vanadium(III) complexes, the Fe^{II}/Fe^{III} and Co^{II}/Co^{III} potentials are similar. The Fe^{II}/Fe^{III} potentials in Table 2 are much more positive than the corresponding potentials found for the $[Fe(entnim)(H^+)_2]^{2+}$ and $[Fe(entnim)FeCl]^+$ complexes (Table 1). This difference probably reflects structural differences where, at least for the $[Fe(entnim)(H^+)_2]^{2+}$ and $[Fe(entnim)(\mu\text{-}Cl)VCl]^+$ comparison, the former almost certainly has the symmetrical structure **5**[8−13] and, as we show presently, the latter has a highly distorted structure. When vanadyl is present in the open site, both complexes (Table 2) show a marked positive increase in the redox potentials of the respective metals in the closed site.

Table 2. Redox Potentials and Peak Separations for the Fe^{III}/Fe^{II} and Co^{III}/Co^{II} Couples for Bimetallic Complexes of the entnim Ligand[a,b]

complex	E_f, V	$E_{pa} - E_{pc}$, V
$[Fe(entnim)(\mu\text{-}Cl)VCl]PF_6$	+0.04	(irreversible)
$[Fe(entnim)VO](PF_6)_2$	+0.69	0.077
$[Co(entnim)VCl_2]PF_6$	+0.44	0.056
$[Co(entnim)VO](PF_6)_2$	+0.94	0.190

[a] Conditions: 5×10^{-4} M sample, 0.1 M *n*-Bu_4NPF_6 in CH_3CN; Pt button working electrode; Pt wire auxiliary electrode; $Ag/AgNO_3$ nonaqueous reference electrode. [b] Potentials are reported relative to the ferrocenium/ferrocene (fc^+/fc) couple as an internal standard which is assigned a value of 0.00 V.

3. Crystal Structures. Crystal data are listed in Table 3 for crystals of $[Fe(entnim)(\mu\text{-}Cl)VCl]PF_6$·$0.3Et_2O$ and of $[Fe(entnim)VO](PF_6)_2$. Selected bond lengths and bond angles for the two structures are listed in Tables 4 and 5. The crystal structure of the ion, $[Fe(entnim)(\mu\text{-}Cl)VCl]^+$, is shown in Figure 1. This structure has two interesting features. First, a chloro bridge exists spanning the two metals. As a consequence, one of the phenolate oxygen atoms (O(2)) is not bonded to the iron

(17) (a) Gerloch, M.; Lewis, J.; Mabbs, F. E.; Richards, A. *J. Chem. Soc. A* **1968**, 112−6. (b) de Vries, J. L. K. F.; Trooster, J. M.; de Boer, E. *J. Chem. Soc., Dalton Trans.* **1974**, 1771−7.

(18) VonDreele, R. B.; Fay, R. C. *J. Am. Chem. Soc.* **1972**, *94*, 7935−6.

Table 3. Crystal Data for [Fe(entnim)(μ-Cl)VCl]PF_6·0.3Et_2O (I) and [Fe(entnim)VO]$(PF_6)_2$ (II)

formula	$C_{35}H_{38}N_6O_2Cl_2PF_6FeV$·0.3$Et_2O$ (**I**)	$C_{35}H_{38}N_6O_3P_2F_{12}FeV$ (**II**)
fw	919.61	987.44
space group	*Cc*	*Pbca*
a, Å	28.881(4)	14.791(3)
b, Å	10.265(1)	20.350(7)
c, Å	17.184(3)	27.059(4)
β, deg	122.73(1)	
V, Å^3	4286(2)	8144(3)
Z	4	8
cryst color	red block	black block
D(calc), g cm^{-3}	1.425	1.611
μ(Mo Kα), cm^{-1}	7.84	7.63
temp, K	298(2)	298(2)
radiation	Mo Kα ($\lambda = 0.710\ 73$ Å)	
$R(F)$,[a] %	6.33	5.56
$R(wF)^2$,[b] %	13.56	11.06

[a] Quantity minimized $= R = \sum\Delta/\sum(F_0)$, $\Delta = |(F_o - F_c)|$; $R(wF)^2 = \sum[w(F_o^2 - F_c^2)^2]/\sum[(wF_o^2)^2]^{1/2}$

Table 4. Selected Bond Distances and Angles of [Fe(entnim)(μ-Cl)VCl]PF_6·0.3Et_2O (I)

Bond Distances (Å)			
Fe−V	3.255	V−Cl(1)	2.286(4)
Fe−Cl(2)	2.440(3)	V−Cl(2)	2.561(4)
Fe−O(3)	2.167(7)	V−O(2)	1.891(8)
Fe−N(3)	2.308(11)	V−O(3)	1.962(7)
Fe−N(4)	2.215(11)	V−N(1)	2.088(9)
Fe−N(5)	2.263(10)	V−N(2)	2.086(11)
Fe−N(6)	2.179(12)	O(2)−C(1)	1.311(9)
		O(3)−C(18)	1.346(8)

Bond Angles (deg)			
Fe−Cl(2)−V	81.19(10)	V−O(3)−Fe	103.9(3)
O(3)−Fe−Cl(2)	81.1(2)	O(2)−V−Cl(1	95.4(3)
N(3)−Fe−Cl(2)	112.1(3)	O(3)−V−Cl(1)	95.2(2)
N(4)−Fe−Cl(2)	163.1(3)	N(1)−V−Cl(1)	97.1(3)
N(5)−Fe−Cl(2)	95.5(3)	N(2)−V−Cl(1)	89.3(3)
N(6)−Fe−Cl(2)	96.9(4)	Cl(1)−V−Cl(2)	177.11(14)
O(3)−Fe−N(3)	116.5(4)	O(2)−V−Cl(2)	83.6(3)
O(3)−Fe−N(4)	83.1(4)	O(3)−V−Cl(2)	82.0(2)
O(3)−Fe−N(5)	168.7(4)	N(1)−V−Cl(2)	85.6(3)
O(3)−Fe−N(6)	85.9(3)	N(2)−V−Cl(2)	91.5(3)
N(4)−Fe−N(3)	80.3(4)	O(2)−V−N(1)	90.6(4)
N(5)−Fe−N(3)	74.7(4)	O(2)−V−N(2)	172.4(4)
N(6)−Fe−N(3)	145.1(4)	O(2)−V−O(3)	85.6(3)
N(4)−Fe−N(5)	98.8(4)	O(3)−V−N(1)	167.4(3)
N(6)−Fe−N(4)	76.1(5)	O(3)−V−N(2)	88.0(4)
N(6)−Fe−N(5)	83.9(4)	N(2)−V−N(1)	94.8(4)
C(18)−O(3)−Fe	120.3(6)	C(1)−O(2)−V	128.5(6)
		C(18)−O(3)−V	128.0(6)

atom. This structural motif has been observed before with this[8] and a related ligand.[19] Second, the pyridine ligands are cis disposed so that the iron atom is coordinated in a distorted octahedral structure. The vanadium atom is also in an octahedral environment, which is less distorted than for the case of the iron atom. The other bond angles and the bond lengths are unexceptional (Table 4). The crystal structure of the ion [Fe(entnim)VO]$^{2+}$ is shown in Figure 2. As in the previous structure, the pyridine ligands are cis disposed, but in this case, both phenolate oxygen atoms bridge both metals. The V−O bond is directed "trans" to the cis pyridine ligands. As in the previous structure, the iron atom is in a distorted octahedral structure. The vanadium aton is 5-coordinate. The bond lengths are "normal", as are the bond angles not directly associated with the iron atom (Table 5).

(19) Diril, H.; Chang, H.-R.; Zhang, X.; Larsen, S. K.; Potenza, J. A.; Pierpont, C. G.; Schugar, H. J.; Isied, S. S.; Hendrickson, D. N. *J. Am. Chem. Soc.* **1987**, *109*, 6207−8.

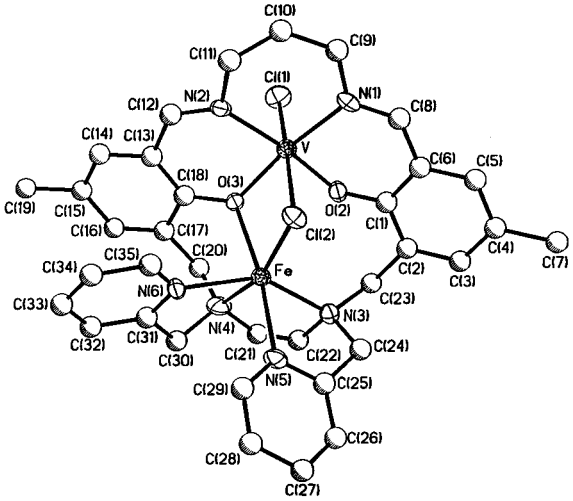

Figure 1. Top view of the molecular structure of [Fe(entnim)(μ-Cl)-VCl]PF_6·0.3Et_2O (**I**).

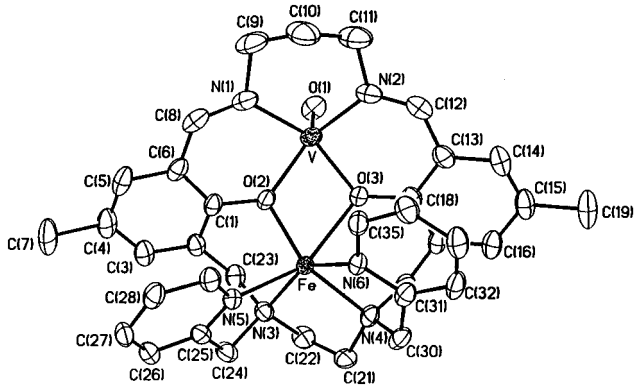

Figure 2. Top view of the molecular structure of [Fe(entnim)VO]-$(PF_6)_2$ (**II**).

Table 5. Selected Bond Distances and Angles of [Fe(entnim)VO]$(PF_6)_2$ (II)

Bond Distances (Å)			
Fe−V	3.289	V−O(1)	1.575(3)
Fe−O(2)	2.069(3)	V−O(2)	1.943(3)
Fe−O(3)	2.251(3)	V−O(3)	1.954(3)
Fe−N(3)	2.217(3)	V−N(1)	2.084(4)
Fe−N(4)	2.185(3)	V−N(2)	2.073(4)
Fe−N(5)	2.195(3)	O(2)−C(1)	1.358(5)
Fe−N(6)	2.164(4)	O(3)−C(18)	1.348(5)

Bond Angles (deg)			
O(2)−Fe−N(3)	89.05(13)	O(1)−V−O(2)	112.4(2)
O(2)−Fe−N(4)	139.48(13)	O(1)−V−O(3)	112.5(2)
O(2)−Fe−N(5)	93.47(12)	O(1)−V−N(2)	102.4(2)
O(2)−Fe−N(6)	121.69(13)	O(1)−V−N(1)	101.9(2)
O(2)−Fe−O(3)	65.85(10)	O(2)−V−O(3)	74.28(11)
N(3)−Fe−O(3)	122.83(13)	O(2)−V−N(1)	85.49(14)
N(4)−Fe−O(3)	86.82(12)	O(2)−V−N(2)	144.6(2)
N(5)−Fe−O(3)	149.13(12)	O(3)−V−N(1)	144.6(2)
N(6)−Fe−O(3)	79.97(12)	O(3)−V−N(2)	86.94(14)
N(4)−Fe−N(3)	81.16(13)	N(2)−V−N(1)	93.8(2)
N(5)−Fe−N(3)	76.85(13)	V−O(2)−Fe	110.12(13)
N(6)−Fe−N(3)	148.57(14)	V−O(3)−Fe	102.70(12)
N(4)−Fe−N(5)	121.76(14)	C(1)−O(2)−V	130.3(3)
N(6)−Fe−N(4)	78.79(14)	C(1)−O(2)−Fe	117.4(3)
N(6)−Fe−N(5)	93.53(13)	C(18)−O(3)−V	131.1(3)
		C(18)−O(3)−Fe	121.5(3)

4. Conclusion. It is shown that in these bimetallic complexes the redox potential of one metal is strongly influenced by the presence of the other. This two-metal deactivation is a consequence of the metals residing in the binucleating ligands because the two coordination sites would be expected to allow

for ready oxidation of the metals in the corresponding monometallic complexes. As was discussed previously,[13] three possible forms of deactivation may operate in multimetallic systems, namely, mechanical coupling where conformational reorganization associated with metal oxidation causes deactivation, through-bond coupling[20] involving electronic interaction of the metals via the bridging ligands, and unfavorable charge−charge interactions between contiguous metals. It is not easy to separate these factors, but the accumulated evidence of this and previous work indicates that mechanical coupling may be the major factor in deactivating two-metal oxidation in the present systems.

Experimental Section

Conductance measurements were made at 25 °C with a YSI Model 35 conductance meter on 0.001 M CH_3CN solutions of the complexes. Infrared spectra were recorded as Nujol mulls on a Nicolet 20 SXB FTIR spectrometer. The UV/vis solution spectra were obtained on a Varian (Cary) 2400 spectrophotometer or on a Perkin-Elmer Lambda 6 spectrophotometer using spectral grade CH_3CN. Magnetic susceptibilities were measured on powdered samples using a Johnson-Mathey-Evans magnetic susceptibility balance. Cyclic voltammograms were recorded using a Bioanalytical Systems BAS 100 electrochemical analyzer on deaerated CH_3CN solutions which were 0.1 M in *n*-Bu_4NPF_6 supporting electrolyte and 5×10^{-4} M in sample. Redox couples were measured using a Pt button working electrode, a $Ag/AgNO_3$ nonaqueous reference electrode, and a Pt wire auxiliary electrode and are tabulated versus a ferrocene standard ($fc^+/fc = 0.0$ V). Cyclic voltammograms on the two complexes $[Fe(entnam)(H^+)_2](PF_6)_2$ and $[Fe(tntnam)(H^+)_2](PF_6)_2$ were recorded using an EG&G Princeton Applied Research Model II electrochemical analyzer equipped with a glassy carbon working electrode and a silver wire reference electrode. All other conditions were identical. Ethanol refers to absolute ethanol. Acetone was dried over 4 Å molecular sieves. The liquid reagents CH_3CN, Et_3N, and DBU[16] used in the synthesis of the bimetallic complexes were each distilled twice over CaH_2. 2,4,6-Trimethyliodosobenzene was prepared by the published method.[21] All preparations of Fe(II) and V(III) complexes were conducted under Ar using deaerated solvents and standard Schlenk techniques. All complexes are air stable as solids unless denoted otherwise. The preparation of the complexes $[Li_2(enal)]$, $[Li_2(tnal)]$, $[Co(entnim)(H^+)_2](PF_6)_2$, $[Fe(entnim)(H^+)_2](PF_6)_2$, and $[Fe(tntnim)(H^+)_2](PF_6)_2$ have been reported previously.[12,13]

$[Fe(tnenim)(H^+)_2](PF_6)_2$. To a mixture of $[Li_2(tnal)]$[13] (0.70 g, 1.2 mmol) and $[FeCl_2(pyridine)_4]$ (0.55 g, 1.2 mmol) was added ethanol (25 mL). The resultant dark brown suspension was stirred for 10 min. To this suspension were added dropwise over 15 min ethylenediamine (84 μL, 1.2 mmol) and acetic acid (450 μL, 7.9 mmol) in ethanol (15 mL). At the end of the addition, all solid material had dissolved. The resultant deep maroon solution was stirred for 1 h, and then NH_4PF_6 (1.0 g, 6.2 mmol) in ethanol (10 mL) was added. A rusty brown solid precipitated immediately. The resultant mixture was stirred for 10 min. The solid was then collected, washed with ethanol (2 × 5 mL), and dried under high vacuum (<0.25 mm). The crude salt was recrystallized from CH_3CN−ethanol. The pure complex $[Fe(tnenim)(H^+)_2](PF_6)_2$ was obtained as brown needles (0.74 g, 64%). $\Lambda_M = 280$ cm^2 Ω^{-1} mol^{-1}. UV [λ_{max} in nm (ϵ in L mol^{-1} cm^{-1})]: 396 (13800), 515 (354, sh), 569 (117, sh), 877 (15). μ_{eff}(25 °C) = 5.3 μ_B. Anal. Calcd for $C_{35}H_{40}N_6O_2P_2F_{12}Fe$: C, 45.56; H, 4.38; N, 9.11. Found: C, 45.54; H, 4.50; N, 8.90.

$[Fe(tntnam)(H^+)_2](PF_6)_2$. To a stirred solution of $[Fe(tntnim)(H^+)_2](PF_6)_2$ (480 mg, 0.512 mmol) in CH_3CN (4 mL) at 0 °C was added dropwise over 15 min a solution of $NaBH_4$ (19.5 mg, 0.512 mmol) in ethanol (8 mL). The yellow-brown color of the imine complex changes to red-brown near the end of the addition. The complex was stirred for 1 h at 0 °C, and the color gradually lightened to red-orange. The solution was then warmed to 60 °C over ∼30 min. Acetic acid (176 μL, 3.07 mmol) was added to the reaction mixture, and a small amount of gas evolution was observed. The resultant orange solution was heated to 100 °C, and water (4 mL) was added, producing a final color change to dark brown. The solvents were slowly distilled from the solution over 30 min until a green microcrystalline solid precipitated. The suspension was cooled to 25 °C over 30 min and then was chilled in an ice bath for 30 min. The solid was collected, washed with water (2 × 5 mL) and ethanol (2 × 5 mL), and was dried under high vacuum (<0.25 mm). The dry solid was extremely air sensitive and was stored in a glovebox. The crude salt (410 mg, 85%) was recrystallized from acetone−ethanol as follows. The green solid (250 mg) was dissolved in acetone (5 mL) at 25 °C, and the brown solution was filtered. To the acetone solution was added ethanol (5 mL). The resultant mixture was heated to 85 °C, and the solvents were slowly distilled from the reaction mixture to induce precipitation. After the solution was reduced to one-half the original volume, the heat was removed and yellow-green crystals precipitated. As the mixture cooled, the crystals grew and the solution developed an intense blue color characteristic of the phenolate−Fe(III) ligand-to-metal charge transfer transition. The mixture was cooled to 25 °C over 40 min and then was chilled in an ice bath for 30 min. The pale green crystals were collected, washed with ethanol (10 mL), and dried under high vacuum (165 mg, 56%). $\Lambda_M = 269$ cm^2 Ω^{-1} mol^{-1}. UV: 303 (7660), 410 (1169) 609 (75), 1048 (11). Anal. Calcd for $C_{36}H_{46}N_6O_2P_2F_{12}Fe$: C, 45.96; H, 4.94; N, 8.94. Found: C, 45.83; H, 4.82; N, 8.65.

$[Fe(entnam)(H^+)_2](PF_6)_2$. To a stirred solution of $[Fe(entnim)(H^+)_2](PF_6)_2$ (595 mg, 0.645 mmol) in CH_3CN (4 mL) at 0 °C was added dropwise over 10 min a solution of $NaBH_4$ (28.0 mg, 0.744 mmol) in ethanol (8 mL). After approximately half of the borohydride solution had been added, a fluffy precipitate formed. The resultant red-brown suspension was stirred for 1.5 h at 0 °C, and the color gradually lightened. The reaction mixture was then warmed to 25 °C. Acetic acid (245 μL, 4.26 mmol) was added to the orange suspension, and a small amount of gas evolution was observed. The mixture was heated to 100 °C for 15 min, and then water (4 mL) was added. The solid dissolved momentarily as the color of the mixture turned deep red-brown, and then a microcrystalline yellow solid precipitated almost immediately. The solvents were slowly distilled from the reaction mixture over 30 min until the total volume was <5 mL. The suspension was cooled to 25 °C over 30 min, and the yellow solid was collected, washed with water (2 × 3 mL) and ethanol (3 × 5 mL), and dried under high vacuum (<0.25 mm). The dry solid was extremely air sensitive and was stored in a glovebox. The crude salt (527 mg, 88%) was recrystallized from acetone−methanol as follows. The yellow solid (450 mg) was dissolved in acetone (25 mL) at 25 °C, and the green-brown solution was filtered. To the acetone solution was added methanol (25 mL). The resultant mixture was heated to 65 °C, and the solvents were slowly distilled from the reaction mixture to induce precipitation. After the solution was reduced to one-half the original volume, yellow crystals formed and the mixture was allowed to cool to 25 °C over 1 h and then to 0 °C over 1 h. The crystals were collected, washed with cold methanol (2 × 5 mL), and then dried under high vacuum (<0.25 mm). The $[Fe(entnam)(H^+)_2](PF_6)_2$ complex (380 mg, 74%) was obtained as yellow needles. $\Lambda_M = 266$ cm^2 Ω^{-1} mol^{-1}. UV: 302 (9835), 434 (922), 599 (120), 1051 (9.5). $\mu_{eff} = 5.1$ μ_B. Anal. Calcd for $C_{35}H_{44}N_6O_2P_2F_{12}Fe$: C, 45.36; H, 4.80; N, 9.07. Found: C, 45.28; H, 4.73; N, 8.80.

$[Fe(entnim)FeCl]PF_6$. To a stirred suspension of $[FeCl_2(pyridine)_4]$ (105 mg, 0.233 mmol) in ethanol (5 mL) was added a red-brown solution of $[Fe(entnim)(H^+)_2](PF_6)_2$ (215 mg, 0.233 mmol) in CH_3CN (2 mL). The color became very dark maroon on mixing. The reaction mixture was heated to 90 °C for 5 min until all solid material had dissolved. The heat was then removed, and dark red crystals precipitated from the solution. The mixture was cooled to 25 °C over 30 min, and then three aliquots of ethanol (5 mL) were added at ∼30 min intervals. The mixture was then allowed to stand for 12 h. The crystals were collected, washed with ethanol (2 × 5 mL), and dried under high vacuum. The crude salt was recrystallized from CH_3CN−ethanol to give red blocks (58 mg, 29%). $\Lambda_M = 127$ cm^2 Ω^{-1} mol^{-1}. UV: 345 (10 150), 515 (907). $\mu_{eff} = 7.1$ μ_B. Anal. Calcd for $C_{35}H_{38}N_6O_2PF_6ClFe_2$: C, 48.49; H, 4.43; N, 9.70; Cl, 4.09. Found: C, 48.22; H, 4.42; N, 9.43; Cl, 3.74.

(20) Hoffmann, R. *Acc. Chem. Res.* **1971**, *4*, 1−9.
(21) (a) Saltzman, H.; Sharefkin, J. G. *Organic Syntheses*; Wiley: New York, 1973; Collect. Vol. V, pp 658−9. (b) Groves, J. T.; Nemo, T. E. *J. Am. Chem. Soc.* **1983**, *105*, 5786−91.

[Fe(entnim)(μ-Cl)VCl]PF_6. The [Fe(entnim)(H^+)$_2$](PF_6)$_2$ complex (500 mg, 0.542 mmol) and VCl_3·3THF (204 mg, 0.542 mmol) were combined in CH_3CN (1.5 mL). To the resultant yellow-brown solution was added Et_3N (151 μL, 1.08 mmol), and the color changed immediately to bright orange. Within 1 min, an orange solid precipitated from the solution. The reaction mixture was stirred for 30 min, and then the solid was collected and washed with Et_2O-CH_3CN (~20:1, 2 × 500 μL) and dried under high vacuum. The orange microcrystalline product (393 mg, 81%) is analytically pure and was used for all subsequent reactions. Crystals suitable for an X-ray crystal structure determination were grown by vapor diffusion of Et_2O into a CH_3CN solution of the complex in an inert atmosphere (Ar). Λ_M = 150 cm^2 Ω^{-1} mol^{-1}. UV: 368 (8570), 505 (1140, sh), 740 (61.5, sh), 1172 (2). μ_{eff} = 5.5 μ_B. Anal. Calcd for $C_{35}H_{38}N_6O_2PF_6Cl_2FeV$: C, 46.83; H, 4.28; N, 9.37; Cl, 7.90. Found: C, 46.71; H, 4.63; N, 9.39; Cl, 7.88.

Reactivity Studies. 1. Reactions with 2,4,6-Trimethyliodosobenzene. A. [Fe(entnim)(μ-Cl)VCl]PF_6 + 2,4,6-Trimethyliodosobenzene. To an orange suspension of [Fe(entnim)(μ-Cl)VCl]PF_6 (99.7 mg, 0.111 mmol) in CH_3CN (750 μL) was added 2,4,6-trimethyliodosobenzene (29.1 mg, 0.111 mmol) under a flow of Ar. The solid was washed down the sides of the reaction vessel with CH_3CN (250 μL). The mixture was stirred for 15 min, and the color slowly darkened as the solids dissolved. The resultant blue-green solution was stirred for 1 h, and then it was exposed to the atmosphere and filtered through Celite. A filtered solution of NH_4PF_6 (0.10 g, 0.60 mmol) in ethanol (10 mL) was added to the reaction mixture. The resultant cloudy mixture was slurried in ethanol (10 mL), and sonication produced a green powder, which was collected, washed with ethanol (2 × 3 mL), Et_2O (2 × 3 mL), and pentane (2 × 3 mL), and dried under vacuum. The crude salt (77.6 mg, 71%) was recrystallized from CH_3CN−ethanol. The [Fe(entnim)VO](PF_6)$_2$ complex was obtained as green needles (60.3 mg, 55%). The dry complex is air stable, although it decomposes over several weeks in CH_3CN solution. Crystals suitable for an X-ray structure determination were grown by vapor diffusion of methanol into a CH_3CN solution of the complex in an inert atmosphere (N_2). Λ_M = 283 cm^2 Ω^{-1} mol^{-1}. IR (V=O stretch): 1014 cm^{-1}. UV: 355 (5650), 555 (51), 608 (55). μ_{eff} = 5.4 μ_B. Anal. Calcd for $C_{35}H_{38}N_6O_3P_2F_{12}FeV$: C, 42.39; H, 4.28; N, 8.48. Found: C, 42.49; H, 3.96; N, 8.40.

B. [Co(entnim)VCl_2]PF_6 + 2,4,6-Trimethyliodosobenzene. The [Co(entnim)(H^+)$_2$)](PF_6)$_2$ complex (100 mg, 0.108 mmol) and VCl_3·3THF (40.5 mg, 0.108 mmol) were combined in CH_3CN (500 μL). To the resultant dark brown solution was added Et_3N (30.2 μL, 0.217 mmol). Within 1 min, an orange solid precipitated from the solution. The reaction mixture was stirred for 15 min, and then the solid was collected, washed with Et_2O-CH_3CN (~4:1, 1 × 2 mL) and Et_2O (1 × 5 mL), and dried under high vacuum. The [Co(entnim)VCl_2]PF_6 product was obtained as an orange powder (49.9 mg, 51%). To an orange suspension of [Co(entnim)VCl_2]PF_6 (49.9 mg, 55.4 μmol) in CH_3CN (500 mL) was added 2,4,6-trimethyliodosobenzene (14.5 mg, 55.4 μmol) under a flow of Ar. The solid was washed down the sides of the reaction vessel with CH_3CN (500 μL). The mixture was stirred for 15 min, and the color slowly darkened as the solids dissolved. The resultant green-brown solution was stirred for 2 h, and then it was exposed to the atmosphere and concentrated to dryness. The green-brown residue was dissolved in DMF (5 mL), and the red-brown solution was filtered through Celite. A filtered solution of NH_4PF_6 (0.45 g, 0.28 mmol) in ethanol (10 mL) was added to the solution. The resultant mixture was diluted with ethanol (40 mL) and Et_2O (30 mL). After 24 h, the brown crystalline product was collected, washed with ethanol (2 × 3 mL), Et_2O (2 × 3 mL), and pentane (2 × 3 mL), and dried under vacuum. Yield: 21.4 mg, 39%. Λ_M = 278 cm^2 Ω^{-1} mol^{-1}. IR (V=O stretch): 1014 cm^{-1}. UV: 357 (5550), 498 (98, sh), 615 (53). Anal. Calcd for $C_{35}H_{38}N_6O_3P_2F_{12}CoV$: C, 42.43; H, 3.87; N, 8.48. Found: C, 42.74; H, 3.90; N, 8.39.

2. Reactions with O_2. A. [Fe(entnim)(μ-Cl)VCl]PF_6 + O_2. To [Fe(entnim)(μ-Cl)VCl]PF_6 (25 mg, 28 μmol) was added CH_3CN (1.00 mL) in a flask open to the atmosphere. The resultant orange solution turned light yellow after ~10 min. After 48 h, the solution was green. A filtered solution of NH_4PF_6 (30 mg, 185 μmol) in ethanol (5 mL) was added to the reaction mixture. After 12 h, ethanol (5 mL) was added to the green solution and crystals formed immediately. The mixture was allowed to stand for 4 h, and then the crystals were collected, washed with ethanol (2 × 3 mL), Et_2O (2 × 3 mL), and pentane (2 × 3 mL), and dried under vacuum. The [Fe(entnim)VO](PF_6)$_2$ complex was obtained as green needles (10.1 mg, 37%). The filtrate was concentrated under reduced pressure, and the blue-green residue was recrystallized from CH_3CN−ethanol to yield a second crop of green crystals (7.1 mg, 26%). Total yield: 63%. The green product has physical properties identical to those of the product described for the reaction with 2,4,6-trimethyliodosobenzene.

B. [Fe(entnim)FeCl]PF_6 + O_2. The [Fe(entnim)FeCl]PF_6 complex (6.75 mg, 7.79 μmol) was dissolved in CH_3CN (7.75 mL), forming a maroon solution. The solution was exposed to air for 5 days. The color did not change during this time. The constancy of the electronic spectrum confirms that the complex did not react with atmospheric O_2 during this time period.

C. [Fe(entnam)FeCl]PF_6 + O_2. The preparation of the diiron(II) complex was carried out in a glovebox. To a stirred golden yellow solution of [Fe(entnam)(H^+)$_2$](PF_6)$_2$ (23.2 mg, 25.0 μmol) in CH_3CN (25 mL) was added DBU (7.5 μL, 50 μmol). The color turned pink immediately. UV: 497 (1800). To the pink solution was added anhydrous $FeCl_2$. As the solid dissolved, the solution developed a salmon-orange color. The mixture was stirred for 15 min, and an aliquot (2.5 mL) was removed for a UV spectrum. UV: 446 (902). The cap was removed from the UV sample, and the solution turned deep blue immediately on exposure. A spectrum was taken 5 min after exposure. UV: 282 (15 260), 335 (9000), 588 (3130).

X-ray Structure Determinations. Crystal, data collection, and refinement parameters are given in Table 3. Suitable crystals were selected and mounted in thin-walled, nitrogen-flushed, glass capillaries. The unit-cell parameters were obtained by the least-squares refinement of the angular settings of 24 reflections ($20° \leq 2\theta \leq 25°$).

The systematic absences in the diffraction data are uniquely consistent for either space group *C2/c* or *Cc* for **I** and *Pbca* for **II**. The *E*-statistics and the absence of a 2-fold axis or an inversion center in the molecule for **I** indicated the non-centrosymmetric space group, which yielded computationally stable and chemically reasonable results of refinement. The structures were solved using direct methods, completed by subsequent difference Fourier syntheses and refined by full-matrix least-squares procedures. Absorption corrections were not required because the variation in the integrated ψ-scan intensities was less than 10%. The Flack parameter refined to −0.01(5) for **I**, indicating that the correct crystallographic enantiomer was determined. There was a partially occupied solvent molecule, diethyl ether, located from the difference map in **I** with a refined occupancy of 30%. All non-hydrogen atoms were refined with anisotropic displacement coefficients except for the phenyl rings and the solvent molecule in **I**, which were refined isotropically to conserve data. Hydrogen atoms were treated as idealized contributions, except for the hydrogen atoms on the solvent molecule in **I**, which were ignored.

All software and sources of the scattering factors are contained in the SHELXTL (5.3) program library (G. Sheldrick, Siemens XRD, Madison, WI).

Acknowledgment. The authors are grateful to Professor Lawrence Sita for the use of his glovebox and electrochemical apparatus. This work was supported by grants from the NSF.

Supporting Information Available: Tables of detailed crystallographic data, atomic coordinates, complete bond lengths and angles, anisotropic displacement coefficients, and hydrogen atom coordinates for **1** and **2** (16 pages). Ordering information is given on any current masthead page.

IC9609923